

Fabrication and Magnetic Properties of Cobalt-Copper Nano-Composite

N. M. Deraz^{1,2,*}, Moustafa M. G. Fouda^{3,4}

¹ Chemistry Department, College of Science, King Saud University, P.O. Box 2455, Riyadh 11451, Saudi Arabia.

² Physical Chemistry Department, Laboratory of Surface Chemistry and Catalysis, National Research Center, Dokki, Cairo, Egypt.

³ Petrochemical Research Chair, Chemistry Department, College of Science, King Saud University, P.O. Box 2455, Riyadh 11451, Saudi Arabia

⁴ Textile Research Division, National Research Center, Dokki, Cairo, Egypt, P.O. Box 12622, Giza 12522, Egypt.

*E-mail: nmderaz@yahoo.com

Received: 5 December 2012 / *Accepted:* 7 January 2013 / *Published:* 1 February 2013

Co/Cu nano-composite was prepared by combustion method. The final product was characterized by X-ray diffraction (XRD). The different magnetic parameters of the as prepared composite were determined by using vibrating sample magnetometer (VSM). The investigated preparation method resulted to formation of CuO/CoO nano-composite. The results obtained showed that the values of saturation magnetization and the remnant magnetization of CuO/CoO nano-composite were found to be 6.75 and 1.97 emu/g, respectively. However, the value of the coercivity of the as prepared composite was 329.7 Oe. The crystal size of cobalt species involved in the as prepared composite decrease as the cobalt content increases.

Keywords: XRD; SEM, EDX; CuO/CoO nano-composite.

1. INTRODUCTION

A burst of research activity is witnessed in recent years in the area of synthesis and fabrication of different size and shape of metal nano-particles. Nanometer sized particles display many interesting optical, electronic, magnetic and chemical properties yielding applications in biological nanosensors, optoelectronics, nano-devices, nano-electronics, information storage and catalysis [1]. Recently, the magnetic nano-particles have been widely studied due to their potential applications in many technological fields such as targeted drug delivery, data storage, sensors, magnetic resonance imaging

[2, 3]. The multi-layers of magnetic/non-magnetic material combination led to their applications in magnetic read/write heads depending upon the phenomenon of giant magneto resistance (GMR) [4]. The desired magnetic properties of different materials depend upon the particle size, shape, composition and surface chemistry of these materials. Using of particles with super-paramagnetic behavior at room temperature (no remanence along with a rapidly changing magnetic state) is preferred for biomedical applications. Super-paramagnetic particles are used for cell sorting, radiation treatment, drug delivery and gene therapy [5]. These particles have a relatively high magnetic moment with low aggregation so that they can be separated from the suspension during cell sorting at relatively low fields. Also, the self-assembly of ferromagnetic particles are used for high-density magnetic media depending upon high saturation magnetization and high coercivity [6].

Composites of transition metal oxides have different applications in areas like catalysis, batteries and solar energy conversion [7]. These composites are capable of mutual interactions leading to the formation of complex structure. So, the properties of transition metal oxides based composites are usually good relative to that of their individual oxide components. Copper and copper compounds are the most important materials [8]. Copper oxides attract the most attention because of their wide spread applications such as thin- film oxygen pressure sensors, binder in pastes for thick-film microelectronic circuits and p-type semiconductor. Moreover, Cu oxides exhibit luminescence [9, 10]. But the most important application of copper oxide particles is as high surface area catalysts that are used in diverse experimental and industrial processes [11-13]. Cobalt and its compounds have found a wide range of applications in super-alloy, magnetic materials, chemical catalyst, battery, cemented carbide and diamond tools. Cobalt nano-particles are expected to possess exceptionally high-density magnetic property, sintering reactivity, hardness levels, excellent impact resistance properties [14-18].

To seek insights into developing new materials, the solid state reactions between the different materials have been studied to explore the advantages of these reactions. The enhancement of these reactions is controlled by thermal diffusion of the reacting materials through the early new compound film which covers the surfaces of grains of reacting materials and acts as energy barrier. There are different affect these reactions such as the precursor compounds, preparation method and preparation conditions [19, 20]. Cobalt oxide-based materials, such as Co-Cu composites, have been widely used for energy storage systems, electro-chromic thin films, magneto -resistive devices and heterogeneous catalysis [21]. The phenomenon of GMR has been observed in the Co-Cu nano-composites [4]. The solid state reaction in the composite of Co- Cu oxides results in the formation of complex structures of spinel or perovskite type [22].

In the current study, we aim to prepare CoO/CuO nano composite via glycine-assisted combustion method and examining its structural and magnetic properties.

2. EXPERIMENTAL

2.1. Materials

Two samples of CoO/CuO composite were prepared by mixing calculated proportions of copper and cobalt nitrates with a certain amount of glycine. The mixed precursors were concentrated in

a porcelain crucible on a hot plate at 350 °C for 10 minutes. The crystal water was gradually vaporized during heating and when a crucible temperature was reached, a great deal of foams produced and spark appeared at one corner which spread through the mass, yielding a brown voluminous and fluffy product in the container. In our experiment, the ratio of the glycine: copper: cobalt nitrates were 4: 1: (1, 2) for S1 and S2 samples, respectively. The chemicals employed in the present work were of analytical grade supplied by Prolabo Company.

2.2. Techniques

An X-ray measurement of various mixed solids was carried out using a BRUKER D8 advance diffractometer (Germany). The patterns were run with Cu K_{α} radiation at 40 kV and 40 mA with scanning speed in 2θ of $2^{\circ} \text{ min}^{-1}$.

The crystallite size of CoO present in the investigated solids was based on X-ray diffraction line broadening and calculated by using Scherrer equation [23].

$$d = \frac{B\lambda}{\beta \cos \theta} \quad (1)$$

where d is the average crystallite size of the phase under investigation, B is the Scherrer constant (0.89), λ is the wave length of X-ray beam used, β is the full-width half maximum (FWHM) of diffraction and θ is the Bragg's angle.

The magnetic properties of the investigated solids were measured at room temperature using a vibrating sample magnetometer (VSM; 9600-1 LDJ, USA) in a maximum applied field of 15 kOe. From the obtained hysteresis loops, the saturation magnetization (M_s), remanence magnetization (M_r) and coercivity (H_c) were determined.

3. RESULTS

3.1. Structural analysis

The XRD patterns of S1 and S2 samples for cobalt in copper matrix with different weight compositions of Co and Cu species are shown in Fig. 1.

Inspection this figure revealed that: (i) The S1 sample consisted of CuO (Monoclinic) and CoO (Cubic) phases. The major phase in the S1 sample is Co oxide with moderate crystallinity. Indeed, the cobalt element has long been known to have two stable crystal line structures: close-packed hexagonal (hcp) and face-centered cubic (fcc). Both phases can exist at room temperature. The fcc structure is thermodynamically preferred above 450 °C and the hcp phase is favored at lower temperatures. For small particles, however, the fcc structure appears to be preferred even below room temperature [24]. But the cobalt species settle in the fcc crystal structure due to the presence of the crystalline copper matrix [25]. (ii) The S2 sample consisted entirely of CoO phase. No additional peak of the second

phase (CuO) was observed in the XRD pattern. This observation speculated that the S2 specimen consisted of single cobalt phase. (iii) In the XRD pattern for the S2 sample, the diffraction peaks related to CoO become sharp and their intensities increase as the cobalt content increases, revealing an increase of the size of Co species involved in the CoO/CuO composite. But, opposite behavior was observed in this study. In other words, the increase in the cobalt content led to decrease in the crystallite size of CoO species with subsequent disappearance of the diffraction lines related to CuO phase.

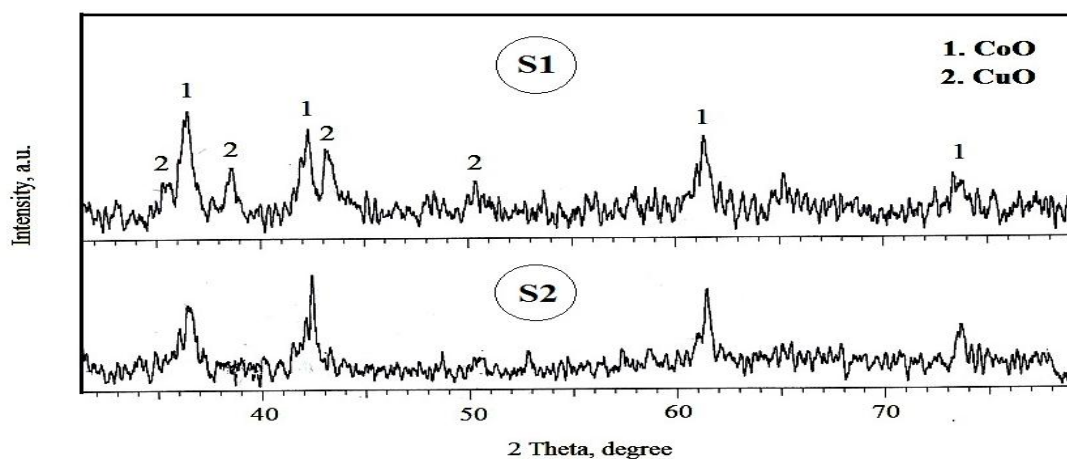


Figure 1. XRD pattern for the S1 and S2 samples.

3.2. The size control of Co nano- crystals

In general, the propellant chemistry containing combustion route can also be chosen to control the nano- crystal size. Adjusting the preparation temperature, the metal precursor- to-fuel ratio and type of both the main fuel and precursor can control the size of nano- particles. Higher temperatures and larger metal precursor-to-fuel ratios produce larger nano- particles [26, 27]. The success of the process is due to an intimate blending among the constituents using a suitable fuel or complexing agent in an aqueous medium and an exothermic redox reaction between the fuel and oxidizer [27, 29]. In this study, we have used glycine as fuel and a mixture of copper and cobalt nitrates followed by heating at 350 °C for 10 minutes to control particle growth. Fuelling of the combustion process achieved by ammonium nitrate produces from combination of nitrate and ammonium ions liberated from decomposition of the reactants [30]. The released heat and gases during the combustion process helps in crystallization and formation of nano- crystals with less agglomeration due to the dissipation of this heat through the whole mass investigated [31,32].

Judicious adjustment of the released heat and gases via the preparation temperature and the metal precursor- to-fuel ratio can control the size of nano- crystals. Indeed, the change in the ratio of glycine to metal nitrates by increasing the cobalt content resulted in a decrease in the crystal size of cobalt nano- particles as shown in Table 1.

Also, Table 1 displays the lattice constant (a), unit cell volume (V) and X-ray density (D_x) of cobalt nano- particles depending upon the data of X-ray. As the amount of cobalt species increases as

the value of lattice constant and unit cell volume of these species increase. Opposite behavior was observed for X-ray density of cobalt nano-particles due to the difference in the atomic weight of both copper (63.54 a.m.u.) and cobalt (58.93 a.m.u.). So, the incorporation of Cu ions in the lattice of Co ions brought about a decrease in the D_x value of Co species with subsequent contraction in their lattices depending upon the difference in the ionic radii. These findings speculated that the crystallite size of cobalt species decreases as the cobalt content increases.

Table 1. Some structural parameters of the as-prepared solids.

Composites	CoO			
	d (nm)	a (nm)	V (nm ³)	D_x (g/cm ³)
S1	21	4.2671	77.6960	6.43
S2	18	4.2620	77.4177	6.45

3.3. Formation of Co- Cu compound

The spinel-type Co_3O_4 and its derivatives such as CuCo_2O_4 are presently being considered as the most promising electrode materials for different reactions such as oxygen evolution, electro-organic preparations and automobile pollution control [10]. Copper oxide substituted cobaltic oxide ($\text{Cu}_x\text{Co}_{3-x}\text{O}_4$) materials can be prepared via solid state reaction between CuO and Co_3O_4 [33]. Recently, these materials were produced by different methods such as thermal decomposition, chemical spray pyrolysis, and sol-gel [33]. Various factors affect the thermal diffusion of Cu and Co cations through the early copper cobaltite film which covers the surfaces of grains of reacting oxides and acts as energy barrier. These factors are the precursor compounds, preparation method and preparation conditions. This is the first study which indicates that the glycine based combustion route can be used to prepare of copper- cobalt compounds.

The enhancement effect of combustion route by using glycine on formation of CuCo_2O_4 was better investigated by measuring the height of certain diffraction lines characteristic for CoO (0.213 nm, 100 %) and relative to one the common lines of both CoO (0.150 nm, 50 %) and CuCo_2O_4 (0.150 nm, 40 %). This was done and the results obtained are given in Table 2.

Inspection of this table revealed that: (i) the ratio, R, between the peak height of the lines at "d" spacing of 0.150 and 0.213 nm for two samples studied was ≈ 0.90 which is greater than that of CoO (0.50). This indicates the formation of CuCo_2O_4 phase by using glycine assisted combustion method. (ii) The increase in the cobalt content led to an increase in the peak height of the lines at "d" spacing of 0.150 and 0.213 nm. The maximum increase in the height of lines at 0.150 and 0.213 nm was 4.3 and 8.5%. Indeed, the disappearance of all the diffraction lines related to CuO and the increase in the peak height of CoO phase which overlaps with that of CuCo_2O_4 phase suggest formation of copper cobaltite

crystallites. However, several authors claimed that the crystallite sizes of CuCo_2O_4 particles are smaller than that of cobalt oxide [34].

Table 2. The effects of cobalt content on the height of some diffraction lines at "d" spacing of 2.13 Å (100 % CoO) and 1.50 Å (50 % CoO, 40 % CuCo_2O_4).

Composites	Peak height (a. u.)		Ratio between b/a (R)
	0.213 nm (a)	0.150 nm (b)	
S1	15.3	13.8	0.90
S2	16.6	14.4	0.87

3.4. Magnetic properties

The hysteresis loop measured for S2 composite is shown in Fig. 2. This sample shows non-zero hysteresis loss at room temperature. The hysteresis loop indicates that the investigated field range is nearly sufficient to saturate the magnetization of cobalt nano-particles.

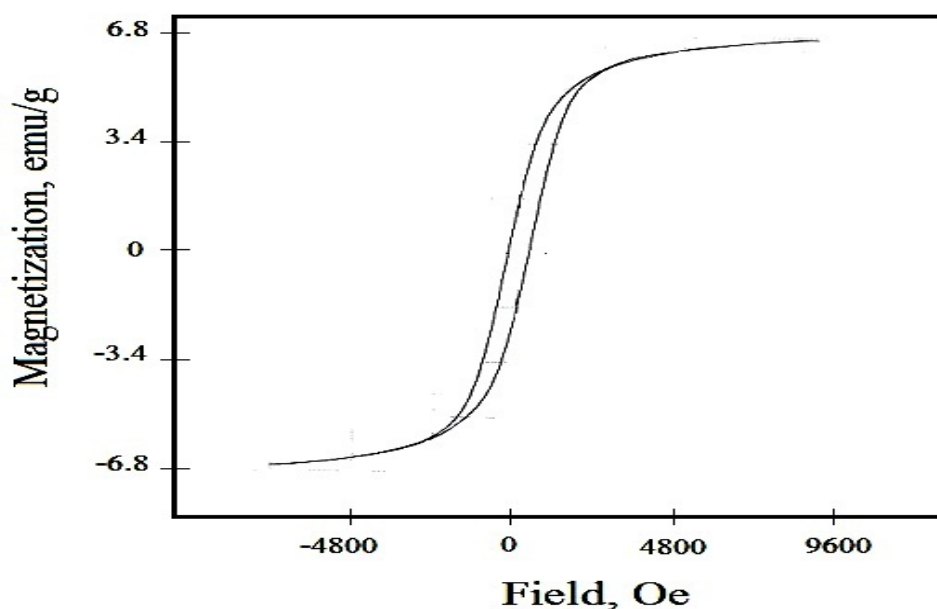


Figure 2. Magnetic hysteresis curves measured at a room temperature for the S2 sample.

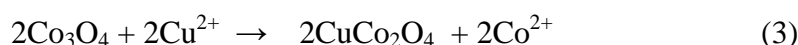
The saturation magnetization (M_s), remanent magnetization (M_r) and the coercivity (H_c) of the S2 sample was determined by measuring the magnetic hysteresis loop at room temperature as shown in Fig. 2. The M_s value was found to be 6.78emu/g and the value M_r was 1.97emu/g for the S2 sample.

The corresponding squareness ratio (M_r/M_s) was found to be 0.29. In addition, the coercivity of the S2 was found to 329.7 Oe.

4. DISCUSSION

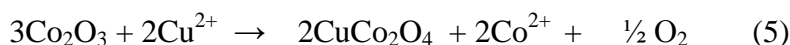
The presence of cobalt species in the crystalline copper matrix resulted in appearance of the fcc crystal structure at temperature greater than the room temperature [25]. In addition, the increase in the cobalt content led to a decrease in the crystal size of cobalt species involved in CoO/CuO composite. The decrease in the crystal size of cobalt species was found to be 14.29 % for the S2 sample due to the increase in the cobalt content. The decrease in the crystallite size of CoO crystallites could be attributed to incorporation of Cu ions in the lattice of Co species with subsequent contraction in this lattice depending upon the difference in the ionic radii of both cobalt and copper. On the other hand, the decrease in the peak height of CoO phase in the S2 sample could be attributed to the solid state reaction between CoO and CuO yielding copper-cobalt compound. Therefore we can control the size of Co nano-crystals by tuning the molar ratio of CoO to CuO.

The dissolution of copper ions in the lattices of cobalt resulted in creation of oxygen vacancies that enhance the mobility of cobalt and copper cations leading the solid solution formation. In addition, the CuO deposits coexist in intimate contact with CoO_x crystallites, favouring oxygen transfer between the two metal oxides. This type of CuO/ CoO_x structure interaction led to an increase in the formation of the Co_2O_3 phase. This indicates the presence of synergistic mechanism between the copper and cobalt oxides. The proposed mechanism in this case is as follows:



In other words, the counter-diffusion of Cu^{2+} and Co^{3+} through a relatively rigid cobaltite film led to the formation of CuCo_2O_4 particles [33, 34]. We speculate that the diffusing ions might be Co^{2+} including Co^{3+} on the basis of detecting Co^{2+} in the interface. In addition, following reactions indicate that Co_2O_3 decomposes to 2Co^{2+} and oxygen gas at Co_2O_3 - interface. Moreover, oxygen moves through the reacted area to be added to the CuO interface and form spinel by reacting with Co^{2+} and CuO:

At Co_2O_3 interface:



At CuO interface:



It is well-known that binary electro-catalyst fabricated from copper and cobalt oxides nanoparticles is proposed as an anode for an amplified electrochemical oxidation of glucose in alkaline medium [35]. In addition, the cobalt nanoparticles in copper matrix show large coercivity which is greater than that of cobalt bulk [2]. Indeed, the magnetization process takes place by rotation of the domain magnetization giving rise to large coercivity. The increase in coercivity could be attributed to the enhanced cubic anisotropy energy which is explained on the basis of percolation and size effects [36]. Kumar *et al.* reported that Co nanoparticles with significant coercivity and anisotropy may be the candidates for the targeted drug delivery when they are prepared in the biocompatible matrices [25]. However, nano-particles of cobalt can be interesting material for magnetic data storage due to high coercivity.

5. CONCLUSIONS

Fabrication of Co- Cu nano-composites via the combustion method by using glycine as fuel has been studied. This method led to formation of solid solution (CuCo_2O_4) through the solid state reaction between cobalt and copper oxides. However, the produced cobalt oxide is in nano-scale size (18- 21nm). The saturation magnetization (6.78emu/g) and coercivity values (329.7 Oe) of the as prepared CoO nano-particles are greater than that for bulk Co crystallites. This increase in the value of coercivity could be attributed the enhanced cubic anisotropy energy depending upon the size effect.

ACKNOWLEDGEMENT

The authors extend their appreciation to the Deanship of Scientific Research at King Saud University for funding this work through research group no RGP- VPP-201.

References

1. D. L. Feldheim and C. A. Foss, Metal nano-particles: Synthesis, characterization and applications (Marcel Dekker Inc.) (eds) 2002 .
2. A. N. Goldstein, Handbook of nano-phase materials, Marcel Dekker Inc., New York, 1977.
3. J. L. Moran-Lopez, J. M. Sanchez, New trends in magnetism, magnetic materials and their applications, Plenum Press, New York, 1994.
4. Julio C. Cezar, Helio C. N. Tolentino, Marcelo Knobel, *Phys. Rev. B* 68(2003)054404.
5. Q. A. Pankhurst, J. Connolly, S. K. Jones, J. Dobson, *J. Phys. D: Appl. Phys.*, 36, R 167-R181, (2003).
6. P. Tartaj, M. P. Morales, S. Veintemillas-Verdaguer, T. Gonzales-Carreno, *J. Phys. D: Appl. Phys.* 36, R182- R197, (2003).
7. Aidong Tang, Huaming Yang, Xiangchao Zhang, *Int. J. Phys. Sci.* 1(2006)101.
8. M. Yin, C. Wu, Y. Lou, C. Burda, J. T. Koberstein, Yimei Zhu, Stephen O' Brien, *J. Am. Chem. Soc.* 127 (2005) 9506.
9. H. Holzschuh and , H. Suhr, *J. Appl. Phys.* A51(1990)486.

10. D. Majumdar, T. A. Shefelbine, T. T Kudas, and H. D. Glicksman, *J. Mat. Res.* 11(1996)2861.
11. D. O.Klenov, , G. N Kryukova,, and L. M. Plyasova, *J. Mat. Chem.* 8(1998)1665.
12. R. Pereira, M. Rufo, and U. Schuchardt, *J. Braz. Chem. Society* 5(1994)83.
13. I. J. Shannon, F.Rey, G. Sankar, J. M. Thomas, T. Maschmeyer, A. M Waller, A. E. Palomares, A. Corma,, A. J. Dent and G. N. Greaves, *J. Chem. Soc. Faraday Trans.* 92(1996)4331.
14. L. Chitu, Y. Chushkin, S. Luby, E. Majkova, A. Šatka, J. Ivan, *Mater Sci. Eng. C* 27(2007)23.
15. P. M. Ivarez, F. J. Beltra'n, J. P. Pocostales, F. J. Masa, *Appl. Catal. B* 72(2007)322.
16. S Liu, K Xu, M Wang, *Int. J. Refract. Met. Hard Mater.* 24(2006)405.
17. H. Shao, Y. Huang, H. S. Lee, Y. J. Suh, C. O. Kim, *J. Magn. Magn. Mater.* 304 (2006) e28.
18. R.N. Singh, J. P. Pandey, N. K. Singh, *Electrochim. Acta* 45(2000)1911.
19. N. M. Deraz, *Ceramics International* 38 (2012) 511.
20. N. M. Deraz, *Ceramics International* 38 (2012) 747.
21. Anjali A. Athawale, Megha Majumdar, Hema Singh, and K.Navinkiran, *Defence Science Journal* 60(2010)507.
22. Jingjuan Wang, Petr A. Chernavskii, Andrei Y. Khodakov, Ye Wa, *J. Catal.* 286 (2012) 51.
23. B.D. Cullity, *Elements of X-ray Diffraction*, Addison-Wesly Publishing Co. Inc. 1976 (Chapter 14).
24. Power diffraction file PDF-2 database sets (1994) pp. 1-44.
25. P Anil Kumar, Subarna Mitra, Kalyan Mandal, *Indian Journal of Pure and Applied Physics* 45(2007)21.
26. N. M. Deraz, A. Alarifi, *Journal of Analytical and Applied Pyrolysis*, 94 (2012) 41.
27. N. M. Deraz, A. Alarifi, *Int. J. Electrochem. Sci.* 7 (2012) 4585.
28. L.C. Pathak, T.B. Singh, S. Das, A. K. Verma, P. Ramachandrarao, *Mater. Lett.*, 57 (2002) 380.
29. J.C.Toniolo, M. D. Lima, A. S. Takimi, C.P. Bergmann, *Mater. Res. Bull.* 40 (2005)561.
30. P. Priyadharsini, A. Pradeep, G. Chandrasekaran, *J. Magn Magn. Mater.* 321(2009)1898.
31. N. M. Deraz, *Current Applied Physics* 12 (2012) 928.
32. N. M. Deraz, *Int. J. Electrochem. Sci.*, 7 (2012) 4608.
33. J. P. Singh, R. N. Singh, *J. New Mat. Electrochem. Systems* 3(2000) 131.
34. Mathieu De Koninck, Simon-Claude Poirier, Benoît Marsan, *J. Electrochem. Soc.*, 153(2006) A2103-A2110.
35. S.M. El-Refaei, M.M. Saleh, M.I. Awad, *Journal of Power Sources* 223 (2013) 125.
36. Gang Xiao, C. L. Chien, *Appl. Phys. Lett.* 51(1987)1280.